Building Serv. Eng. Res. Technol. **11**(3) 87–96 (1990) Printed in Great Britain

#4534

Summary The pair of papers of which this is the second presents some of the commonest methods for calculating long-wave radiation heat exchange in a room. Paper I covered the theory behind the various methods. These vary in complexity from accurate calculation of view factors with multiple inter-reflections between surfaces to simple, non-geometric methods using fixed heat transfer coefficients. This paper (Paper II) presents the results of a set of tests which were developed to compare the performance of these algorithms with an analytically exact method. The main conclusion is that in many cases it is possible to use a non-geometric model without significant loss of accuracy. A more accurate method is required in cases of low surface emissivity or large temperature differences between surfaces. The importance of internal long-wave radiation for the overall energy balance of typical houses was tested, and the results are presented here. If no account is taken of long-wave exchange (disabling exchanges by setting all internal emissivities to zero), predicted energy requirements change by up to −11% in the type of house and heating system tested. Greater changes could arise in different house types or those with a larger radiant output from the heating system. The results also showed the importance of modelling long-wave exchange to and from windows explicitly.

Internal long-wave radiation exchange in buildings: Comparison of calculation methods: II Testing of algorithms

P Stefanizzi† PhD, **A Wilson**‡ PhD and **A Pinney**‡ PhD
† Facultia di Ingegneria, Universita di Bari, Italy
‡ Building Research Establishment, Garston, Watford WD2 7JR, UK

Received 13 June 1989, in final form 17 April 1990

1 Introduction

Paper I[1] presented in detail the theory behind a range of methods for calculating internal long-wave radiation exchange in buildings; this paper tests those methods. Two types of test are presented: (*a*) analytical tests, in which the results from any method are compared with those from a theoretically exact method, for a range of simplified room types; (*b*) tests on real buildings, comparing total annual energy consumption results with internal long-wave exchange 'enabled' with results obtained when it was 'disabled' by setting all internal emissivities to zero. These latter tests are used to assess the importance of errors in the calculation of long-wave exchange on the overall energy balance of a building. The exact method used is by Siegel and Howell[2]; the other methods tested are described briefly below.

1.1 ESP model

Net long-wave gain on each surface is calculated using grey-body radiation coefficients, containing a linearisation for the T^4 term. The most accurate method (ESP(1)) accounts for multiple reflections between all surfaces[3]. Previous time-row surface temperatures are used to calculate current coefficient values, thereby avoiding the need for iteration. In ESP(1) view factors are calculated by a ray tracing method; the 'default' method (ESP(0)) calculates view factors uses a simple area weighting method (only exact for a cube). In an earlier version of ESP (ESP(2)) the radiation coefficient took into account reflections between pairs of surfaces only, so not accounting for possible interactions with other surfaces.

1.2 NBSLD model

NBSLD[4] estimates long-wave radiation using 'radiation exchange factors' which contain the view factor between the surface being considered and that with which it is exchanging radiation, the emissivity of the surface being considered, and a simplification for the surface temperature difference. The program adds the contributions from all surface to obtain the balance on any one surface. The program uses an area ratio to calculate view factors.

1.3 DEROB model

DEROB[5] models long-wave radiation using the 'infrared illumination tensor' matrix $[\mathcal{J}]$. The generic element $\mathcal{J}_{ij}$ of that matrix is the fraction of energy emitted from the *i*th surface which arrives at the *j*th one, accounting for multiple diffuse reflections from all surfaces. View factors are found by substituting an approximate expression for the exact integral one.

1.4 Walton's model

Walton[6] proposes the 'mean radiant temperature (MRT) balance' method. Each surface radiates to a fictitious surface having characteristics (area, emissivity and temperature) derived from those of all other surfaces. (Even surfaces coplanar to the surface being considered are included in the summations, to retain the method's simplicity.) Imbalances in total flux are redistributed by area weighting to achieve energy conservation.

1.5 Davies's model

Davies[7] starts from the Oppenheim formulation of radiative heat exchange in terms of a 'delta' resistance network, and finds values of resistances for the equivalent 'star' network which considers all exchanges to take place through a fictitious star point. The temperature of the star point is derived from the properties of all other surfaces, and by regression analysis on a set of rectangular boxes, and so is strictly only valid for a rectangular cavity with six exchanging surfaces.

1.6 CIBSE model

In the *CIBSE Guide* Section A5[8] heat exchange is calculated using a fictitious temperature called 'environmental temperature'. This accounts for both convective and radiative exchange, and is a function of room dimensions and convective and radiative heat transfer coefficients. The radiative component is calculated as a function of the difference between the temperature of surface i and the mean temperature of all other surfaces.

2 Description of analytical tests

Drawing upon previous experience[6,9], test cases were developed which allow the quantification of errors in the calculation of long-wave radiation by existing models. The important variables are temperature, emissivity and geometric configuration, and in each test only one variable is altered at a time. All tests were steady-state, and Figure 1 shows the geometrics used; exact view factors are calculated analytically.

To conduct worthwhile tests using a full simulation model it would be necessary to 'switch off' all other processes. Most models do not offer this facility, so results would have to be interpreted taking into account other processes/interactions. Any conclusions about the adequacy of internal long-wave exchange would therefore not be very robust. To avoid this problem, the internal long-wave algorithms have been tested in isolation from the models.

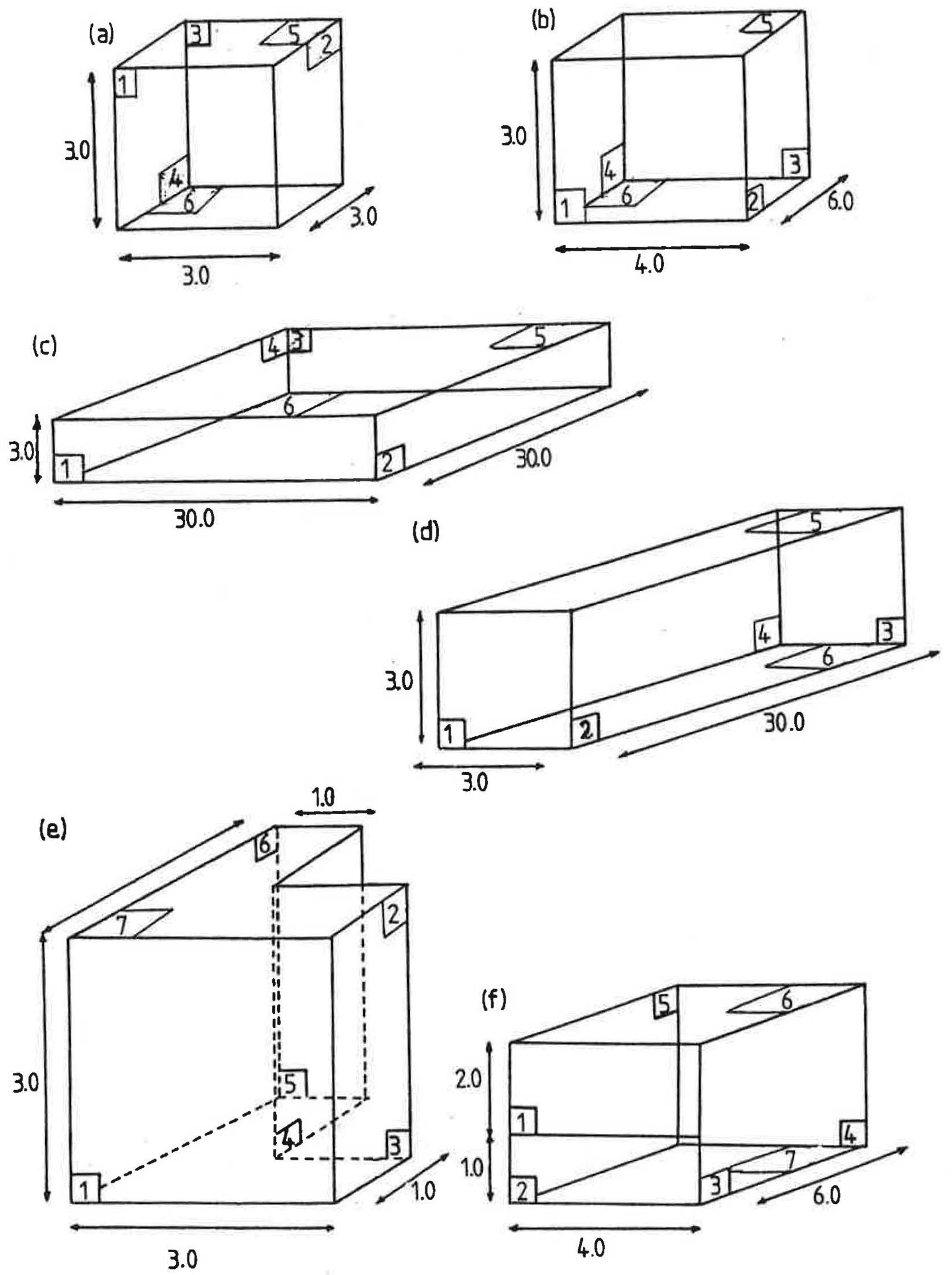

Figure 1 Geometries studied (dimensions in metres)

In Test 1 a cubic geometry (edge = 3 m) is considered, with all surface emissivities set to 0.9, and the radiation fluxes are found for four different temperature distributions likely to be representative of thermal conditions found in practice.

In Test 2 the same cubic geometry is investigated for a single temperature distribution, and the fluxes are computed for various values of emissivity on surface 1.

In Test 3, for constant temperatures and emissivities the energy exchanges in different geometric configurations are determined. Test 2 had already shown the error inherent in the ESP(2) algorithm (which was replaced in the ESP program as a result), so this method was not tested further. In addition, the NBSLD and Davies methods cannot model the L-shaped room, and so were not included in Test 3(e).

In Test 4 a more realistic configuration is considered with a seventh surface. Thus in the (f) configuration (Figure 1) one can either visualise surface 1 as a normal glass window in an external wall (Tests 4(a), 4(b) (but see the limitations on modelling windows using ESP described below) or as a low-emissivity surface (4(c), 4(d)), while surface 2 could represent a radiator (4(b), 4(d)) or a simple opaque wall (4(a), 4(c)).

Table 1 Parameters for Test 1

Geometric configuration (Figure 1)		(a)
Emissivity of all surfaces		0.9
Temperature	Surfaces 2–6	20°C
	Surface 1	−15, 10, 30, 60°C

Table 2 Test 1 results: Net radiant heat flux on surface 1

Temperature (°C)	−15	10	30	60
Test label	1A	1B	1C	1D
Method	Net radiant heat flux on surface 1 (W)			
Exact	1325.8	431.1	−477.5	−2221.5
ESP(1)	1314.6	427.5	−473.5	−2202.9
NBSLD	1641.3	468.9	−468.9	−1875.7
DEROB	1325.8	431.1	−477.5	−2221.6
Walton	1355.7	434.0	−474.2	−2158.8
Davies	1325.8	431.1	−477.5	−2221.5
CIBSE	1616.0	461.7	−461.7	−1846.8
ESP(0)	1314.7	427.5	−473.5	−2202.9
ESP(2)	1325.5	431.0	−477.4	−2221.1

3 Analytical test details and results

3.1 Test 1

None of the energy balances differed from zero. Figure 2 shows the errors from Test 1 of the various models in their calculation of heat flux on surface 1 calculated as:

$$\frac{100(f_m - f_e)}{f_e} \quad (\%) \tag{1}$$

where f_m and f_e are the model and exact heat fluxes respectively.

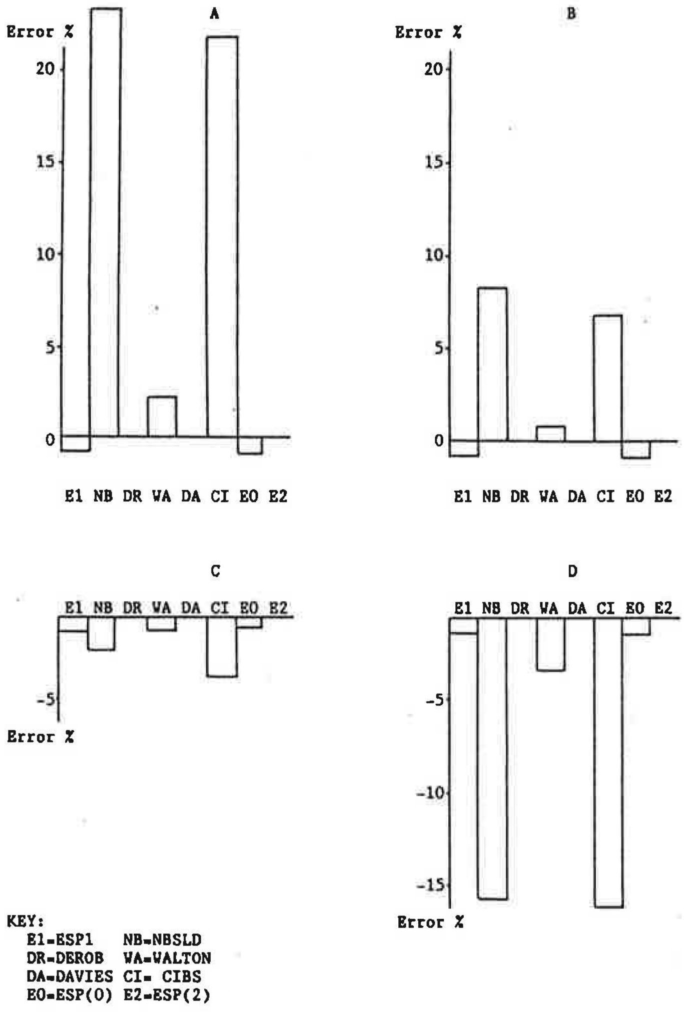

Figure 2 Comparative error graphs for Test 1

3.2 Test 2

The values of heat flux on surfaces 3, 4, 5 and 6 from Test 2 were almost identical to those for surface 2. The errors, shown in Figure 3, are calculated as:

$$\left[\sum_{k=1}^{N} (f_{mk} - f_{ak})^2\right]^{1/2} \tag{2}$$

where f_{mk} is the model flux and f_{ak} the analytical flux for surface k. The accuracy of determination for surface 1 is no longer typical of the accuracy for other surfaces.

3.3 Test 3

Errors are calculated from eqn. (2), and are shown in Figure 4.

3.4 Test 4

Errors for Test 4 are calculated as in Test 2, and shown in Figure 5.

4 Summary of results for analytical tests 1–4

It is worth noting that, in some cases, rounding errors can be significant (for example, it was found necessary to specify exact view factors to at least six decimal places). Such errors could be overcome by adopting double precision in the computer program, but this was not done in this work, as it was considered best to test the different algorithms as they are currently implemented. In some cases the small energy imbalances reported (cf Tests 3 and 4) are due to the finite accuracy of the computer used, rather than to the method itself. This is known to be the case for the Davies method.

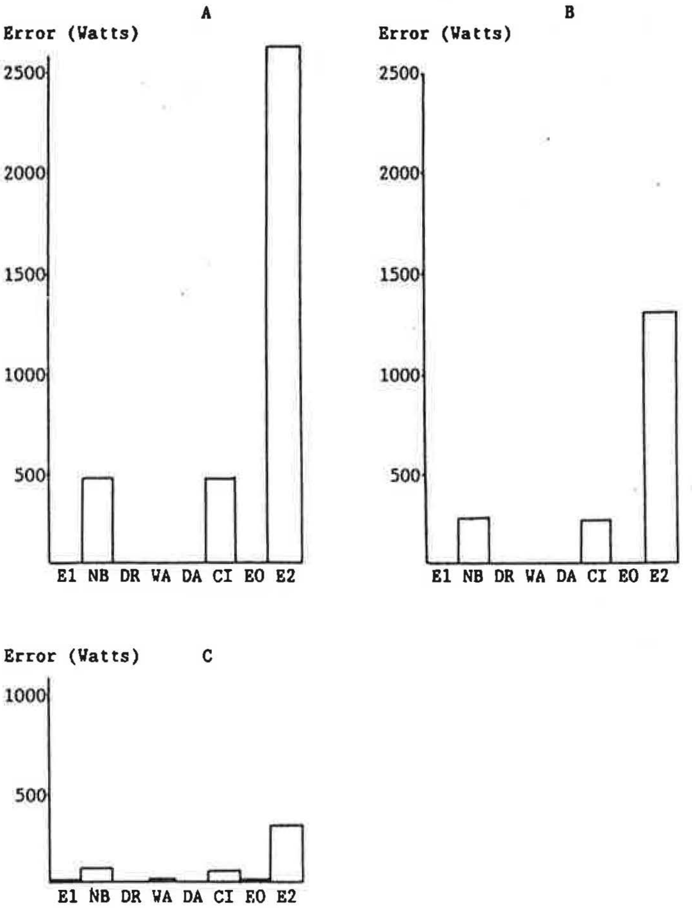

Figure 3 Comparative error graphs for Test 2 (key as Figure 2)

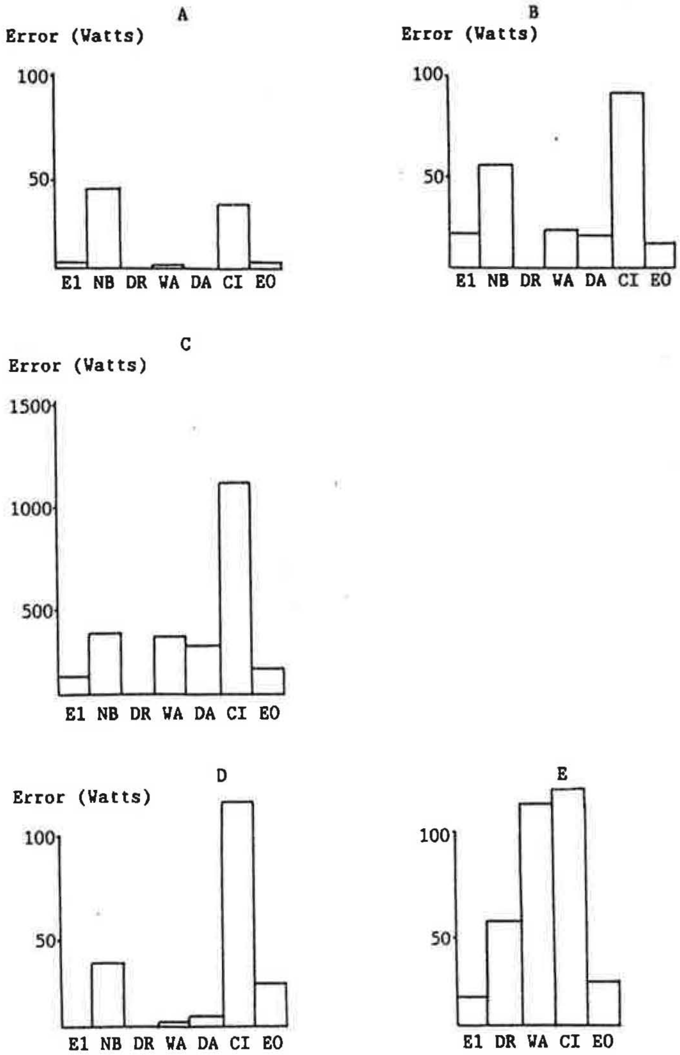

Figure 4 Comparative error graphs for Test 3 (Note different scale for Test 3C) (key as Figure 2)

Table 3 Parameters for Test 2

Geometric configuration (Figure 1)		(a)
Emissivity	Surfaces 2–6	0.9
	Surface 1	0.1, 0.5, 0.8
Temperature	Surfaces 2–6	20°C
	Surface 1	10°C

Table 4 Results for Test 2: Net radiant flux on surfaces 1 and 2

Emissivity of surface 1	0.1	0.5	0.8	0.1	0.5	0.8
Test label	2A	2B	2C	2A	2B	2C
Method	Net radiant heat flux on surface 1 (W)			Net radiant heat flux on surface 2 (W)		
Exact	48.8	241.6	384.0	−9.8	−48.3	−76.8
ESP(1)	47.6	237.8	380.1	−9.6	−47.7	−76.3
NBSLD	468.9	468.9	468.9	−93.8	−93.8	−93.8
DEROB	48.8	241.6	384.0	−9.8	−48.3	−76.8
Walton	50.4	246.2	387.7	−10.1	−49.3	−77.6
Davies	48.8	241.6	384.0	−9.8	−48.3	−76.8
CIBSE	461.7	461.7	461.7	−92.3	−92.3	−92.3
ESP(0)	47.6	237.8	380.1	−9.6	−47.8	−76.3
ESP(2)	2468.6	1448.2	685.0	−495.3	−290.6	−137.5

Table 5 Parameters for Test 3A–D

Emissivity	For all surfaces	0.9
Temperature	Surfaces 2–6	20°C
	Surface 1	10°C

Table 6 Results for Test 3A, geometry (a): Net radiant flux on each surface

Surface	1	2, 4	3	5, 6	Energy balance
Method	Net radiant heat fluxes (W)				
Exact	431.1	−86.2	−86.2	−86.2	0.0
ESP(1)	427.5	−85.8	−84.2	−85.8	0.0
NBSLD	468.9	−93.8	−93.7	−93.8	0.0
DEROB	431.1	−86.2	−86.2	−86.2	0.0
Walton	434.0	−86.8	−86.8	−86.8	0.0
Davies	431.1	−86.2	−86.2	−86.2	0.0
CIBSE	461.7	−92.3	−92.3	−92.3	0.0
ESP(0)	427.5	−85.8	−84.2	−85.8	0.0

Table 7 Results for Test 3B, geometry (b): Net radiant flux on each surface

Surface	1	2, 4	3	5, 6	Energy balance
Method	Net radiant heat fluxes (W)				
Exact	579.0	−113.5	−52.9	−149.5	0.0
ESP(1)	590.3	−118.6	−52.7	−159.3	−18.2
NBSLD	625.3	−123.3	−54.5	−162.1	0.0
DEROB	579.0	−113.5	−52.9	−149.5	0.0
Walton	587.5	−107.3	−67.1	−152.9	0.0
Davies	574.0	−104.2	−65.0	−150.3	0.0
CIBSE	656.6	−123.1	−82.1	−164.2	0.0
ESP(0)	587.3	−118.1	−51.8	−158.8	−18.2

Table 8 Results for test 3C, geometry (c): Net radiant flux on each surface

Surface	1	2, 4	3	5, 6	Energy balance
Method	Net radiant heat fluxes (W)				
Exact	4377.8	−235.5	−117.7	−1894.5	0.1
ESP(1)	4336.3	−254.1	−76.2	−1823.3	105.3
NBSLD	4689.3	−258.0	−116.9	−2028.2	0.1
DEROB	4377.7	−235.5	−117.7	−1894.8	−0.4
Walton	4475.5	−101.1	−101.1	−2086.1	0.0
Davies	4382.4	−121.6	−121.6	−2008.9	−0.1
CIBSE	5309.5	−230.9	−230.9	−2308.6	−0.3
ESP(0)	4327.3	−255.1	−75.0	−1818.4	105.3

Table 9 Results for Test 3D, geometry (d): Net radiant flux on each surface

Surface	1	2, 4	3	5, 6	Energy balance
Method	Net radiant heat fluxes (W)				
Exact	438.6	−109.1	−2.3	−109.1	0.0
ESP(1)	451.3	−120.5	−2.3	−120.4	−32.8
NBSLD	468.9	−116.9	−1.5	−116.9	0.0
DEROB	438.6	−109.1	−2.4	−109.1	0.0
Walton	441.7	−108.4	−8.1	−108.4	0.0
Davies	436.8	−107.1	−8.4	−107.1	0.0
CIBSE	540.9	−131.9	−13.2	−131.9	0.1
ESP(0)	448.5	−119.8	−2.2	−119.8	−32.8

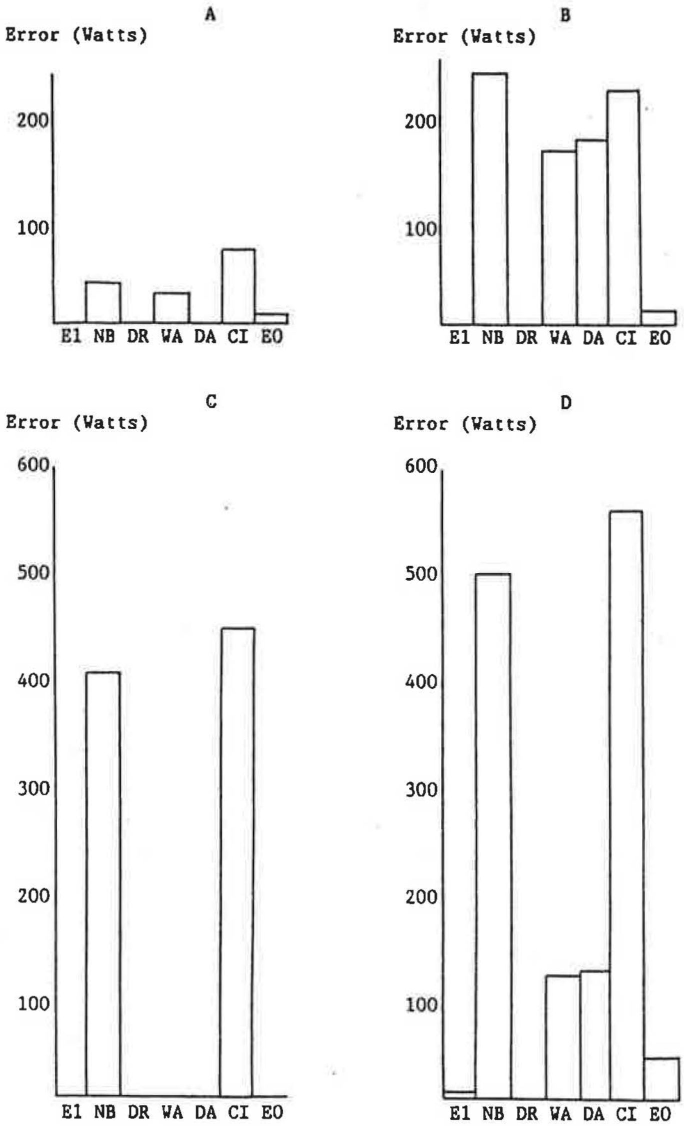

Figure 5 Comparative error graphs for Test 4 (key as Figure 2)

Table 11 Parameters for Test 4

Geometric configuration		(f)
Temperature	Surfaces 3–7	20°C
Emissivity ε	Surfaces 2–7	0.9

Table 10 Results for Test 3E, geometry (e): Net radiant flux on each surface

Emissivity ε for all surfaces 0.9
Temperature All surfaces at 20°C except surface 3 at 10°C

Surface	1	2	3	4	5	6	7	8	Energy balance
Method	Net radiant heat fluxes (W)								
Exact	−153.5	−44.5	284.9	−2.0	−1.3	−15.8	−33.9	−33.9	0.0
ESP(1)	−169.1	−49.4	280.6	−1.9	−0.9	−14.4	−28.5	−28.6	−12.3
DEROB	−155.6	−10.9	285.5	−3.1	−1.6	−40.8	−70.8	−45.4	−42.6
Walton	−69.1	−20.0	291.1	−42.9	−20.0	−69.1	−34.9	−34.9	0.0
CIBSE	−72.3	−24.1	321.2	−48.2	−24.1	−72.3	−40.2	−40.2	0.0
ESP(0)	−171.2	−48.7	286.3	−3.4	−1.7	−14.9	−29.3	−29.3	−12.2

Table 18 Parameters for Test 4D

Temperature	Surface 1	10°C
	Surface 2	60°C
Emissivity ε	Surface 1	0.1

Table 19 Results for Test 4D: Net radiant flux on each surface

Surface	1	2	3, 5	4	6	7	Energy balance
Method	Net radiant heat fluxes (W)						
Exact	44.3	−1002.7	179.6	86.4	160.3	352.5	0.0
ESP(1)	43.5	−986.7	174.4	81.4	156.2	347.7	−9.2
NBSLD	416.8	−833.7	82.2	36.3	108.1	108.1	0.1
DEROB	44.3	−1002.7	179.6	86.4	160.3	352.5	0.0
Walton	54.5	−996.3	172.7	109.2	243.6	243.6	0.0
Davies	51.5	−1026.3	177.0	110.4	255.2	255.2	0.0
CIBSE	529.0	−966.7	82.1	54.7	109.4	109.4	0.0
ESP(0)	43.5	−1048.4	185.8	87.3	169.2	367.6	−9.2

Table 20 Assumed radiation coefficient C for Test 1

Method	Temperature of surface 1 (°C)			
	−15.0	10.0	30.0	60.0
	Constant C ($\text{WK}^{-4} \times 10^7$)			
Exact	−4.503	−4.503	−4.503	−4.503
ESP(1)	−4.465	−4.465	−4.465	−4.465
NBSLD	−5.575	−4.898	−4.422	−3.802
DEROB	−4.503	−4.503	−4.503	−4.503
Walton	−4.605	−4.533	−4.472	−4.376
Davies	−4.503	−4.503	−4.503	−4.503
CIBSE	−5.489	−4.823	−4.354	−3.743
ESP(0)	−4.465	−4.465	−4.465	−4.465
ESP(2)	−4.502	−4.502	−4.502	−4.502

Tests 1A–D were designed to assess temperature-related errors. In these tests, five of the surfaces are isothermal at 20°C; the temperature of the sixth takes four values. Therefore the heat flow between the single surface (1) and the others (2) can be calculated by

$$Q = C(T_1^4 - T_2^4) \tag{3}$$

where C is a constant, having the value $4.503 \times 10^{-7}\,\text{WK}^{-4}$. The values of C 'assumed' by the different methods can be calculated, and these are shown below.

The largest errors come from NBSLD and CIBSE, owing to poor assumptions in the linearisation of the fourth-power law, and also in part to an inbuilt assumption that each surface radiates to a black body. Errors in the equation used to linearise the T^4 term account for the variability in the Walton method, and in part for the errors in the ESP methods. Other errors in the ESP algorithms are due to (*a*) rounding errors in the computer, which could be overcome by working in double precision, and (*b*) the fact that only three-surface interactions are used in the calculation of the radiant transfer coefficient[3]. The results for the Davies and DEROB methods are both identical to the exact results, showing the correctness of their methods for cubic geometries.

Emissivity-related errors were examined in Tests 2A–C and found to be small for all method except NBSLD and CIBSE. In these the errors were large because the methods do not allow emissivity values to be changed. The results for ESP(2) clearly show that this algorithm is incorrect, and was replaced in subsequent versions of ESP by ESP(0) and ESP(1).

Table 21 Monthly heating requirements in the semi-detached house

Month	Test A	Test B	e
	Monthly heating requirement (kWh)		
Jan	1762.3	1696.5	−3.7
Feb	1312.2	1269.5	−3.3
Mar	1041.7	1003.9	−3.6
Apr	906.0	876.5	−3.3
May	455.9	442.8	−2.9
Jun	110.4	106.3	−3.7
Jul	14.0	12.6	−10.0
Aug	62.1	61.3	−1.3
Sep	218.4	214.1	−2.0
Oct	558.0	542.1	−2.8
Nov	1433.3	1389.6	−3.0
Dec	1780.0	1725.9	−3.0
Total	9654.3	9341.1	−3.2

For the non-cubic geometries in Test 3 both ESP(1) and ESP(0) violate the first law of thermodynamics (Tables 6–10). This is most likely accounted for by the following. (*a*) Only flow paths involving no more than three surfaces are considered and thus all are underestimates of the full values. (*b*) The view factors sometimes fail to satisfy reciprocity. (*c*) The above-mentioned rounding errors occur in the computer implementation.

Early results for Test 3 showed a serious error in DEROB in the calculation of view factors. A flag set in the program defines, as the default condition, a time-saving technique different from that explained in the manual. In order to find the view factor F_{ij} it divides the i and j surfaces into nine equal-area pieces and computes F_{ij} as 9 times the quantity

$$F_{nm} = (\mathbf{R}_{nm}\, \Delta A_i)\,(\mathbf{R}_{nm}\, \Delta A_j)/(\mathbf{R}_{nm})^4 \qquad (4)$$

where n is the index of the small central area on surface i, and m is the index of the same one on the j-surface. For all results quoted here the flag was reset so as to follow the method described in the manual. Without this, errors in view factors stretched to 23 000%.

With the above correction, DEROB performed well throughout Test 3 (its energy imbalance in Test 3E is caused by the computer rounding errors mentioned above); as expected, other methods become poorer as the geometry differs more from cubic. The Davies and NBSLD methods do not claim to be able to model the L-shaped room, and even among those methods which can model it, the assumption of uniformly distributed radiation on all surfaces (as set out in Paper I) does not strictly apply in this case, when one surface is partly shaded from another. The results for the L-shaped room should therefore be considered as a comparison of the different methods, rather than as a representation of reality.

In Test 4, which includes the common situation of a window in an external wall, ESP(1) and DEROB gave the best results. Errors similar to those illustrated for the CIBSE method in the above tables must be expected from programs, like SERI-RES[10], which handle radiation by a fixed convection–radiation combined coefficient.

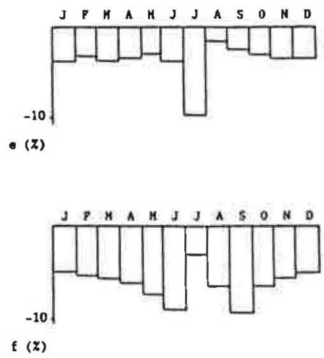

Figure 6 Graphs of errors e and f for the semi-detached house

Table 22 Annual total heating requirements (kWh) in all houses

Building	Test A	Test B	e
Semi	9654.3	9341.1	−3.2
Terrace	5845.1	5968.7	+2.1
Bungalow	7022.0	6880.9	−2.0
Timber frame	5002.3	5031.5	+0.6

Table 23 Annual heating requirements in terraced house, with all party walls treated as external

A	B	e
Annual heat load (kWh)		
8794.1	8586.4	−2.4

5 Tests on standard buildings

The importance of internal long-wave radiation exchanges relative to whole-building performance was tested, using ESP(0) as the model. This choice was made for several reasons, in particular that it is easy to 'switch off' (see below) long-wave exchanges. Buildings used were a semi-detached house, a post-1919 terraced house, a bungalow and a timber-framed terraced house, all typical of the UK building stock[11]. The heating was controlled on the basis of internal air temperature, and heat was input at the air point. Weather data were from Kew for 1967.

As a base for each building, a full year's results A were obtained, shown as twelve one-monthly sets. In the second set of runs B all internal emissivities were set to zero so as to exclude long-wave exchanges. The version of ESP used here treats windows as U-value elements, which have a combined radiative/convective surface coefficient. No attempt was made to modify the U-value to eliminate the radiant component in these tests (but see the improved tests below).

6 Results for standard buildings

In all cases the error e is determined as $100\,(B–A)/A(\%)$, so that this error shows the effect of ignoring internal long-wave radiation.

6.1 Semi-detached house

Results are shown in Table 21 and Figure 6.

The yearly totals for the various buildings were as given in Table 22.

The results from Tests A and B for the given set of buildings suggest that a key feature in determining the effect of removing internal long-wave radiation is the proportion of internal surface area that is part of a wall connected to cold external conditions. This would account for the differences between, for example, the bungalow and the terrace. To test this hypothesis a simple change was made to the description of the terraced house, making all party walls into external walls by changing the 'connection types' in the input file for ESP. The results from this test clearly offer support to the hypothesis.

Finally, to test the effect of using more accurate view factors, the bungalow run was repeated using ESP(1), with accurate view factors calculated using the ray tracing method. The yearly heating requirement was reduced by 0.4% to 6 997 kWh.

7 Improved comparative simulations

All the results presented above were obtained using a version of ESP which did not account explicitly for long-wave radiation between walls and windows, and which treated windows as fixed U-value elements. Current versions of ESP (denoted ESP(3)) allow windows to be modelled as transparent layers, treated in the same way as opaque elements but with the addition of transparent properties. Long-wave radiation to and from windows is also modelled explicitly.

Table 24 Comparison of monthly heating requirements in a typical single-storey house, showing the effects of modelling long-wave exchange to and from windows

Month	Monthly heating requirement (kWh)			
	ESP(0) LW enabled	ESP(3) LW enabled	ESP(0) LW disabled	ESP(3) LW disabled
January	698	659	695	618
February	546	515	529	461
March	437	405	414	339
April	331	308	317	255
May	123	117	121	90
June	4	5	5	3
July	0	0	0	0
August	0	0	0	0
September	9	13	11	8
October	152	154	164	133
November	521	506	528	468
December	709	680	698	623
Total	3530	3362	3482	2998

To assess the importance of this change, a simple two-zone model (corresponding to a typical living area and loft) was modelled using first the original version of ESP (ESP(0)), the improved version (ESP(3)) with long-wave radiation enabled (both methods with view factors calculated using area weighting), and both versions with long-wave switched off. Table 24 shows the variation in monthly heat demand caused by choosing the different methods.

The results show only reasonable agreement between modelling windows as *U*-value elements and the more exact method; the difference in total annual heat requirement is 4.7%, with the largest differences occurring during the winter months.

Of more interest, though, are the differences in energy requirements when LW is disabled in the two methods. When LW exchange to windows is not modelled (ESP(0)), energy demand falls by only 1.4%. However, when LW exchange with windows is modelled, the predicted demand falls by 10.8%. This is far higher than that obtained using the earlier version of ESP, and clearly shows the importance of modelling long-wave exchange with windows explicitly.

The above results were obtained assuming a purely convective heat input. Differences greater than 11% would occur in houses with radiant heaters, or those with a higher proportion of glazing.

8 Conclusions

The main algorithms currently in use in thermal calculation procedures for calculating radiative heat exchange in a room have been reviewed. Tests have been designed which are simple enough to allow analytic solutions to be derived and which are able to exhibit the error source in each numerical model response. Of the methods tested, the ESP(1) (with view factors calculated using ray tracing, but without LW exchange to windows), ESP(3) (with LW exchange to windows), DEROB, Walton and Davies algorithms are able accurately to model rooms in which temperature and emissivity varied between surfaces. However, DEROB shows a serious error in view factor computation when operating in its default condition, and the Walton and Davies algorithms are poor for geometries which differ significantly from the six-sided rectangular shape.

The other methods tested are limited in their accuracy, because of linearisation of the fourth-power temperature law, the incorrect computation of view factors in non-cuboid geometries, or not allowing the emissivity to vary from 0.9.

The results of Buchberg[12] suggest that the algorithm used for long-wave radiation exchange computation does not influence the thermal behaviour of the building or its annual heating requirement very much in normal building structures. Our results, however, do not support this conclusion, and show that internal long-wave exchange can account for 10% of total heat losses. In addition, they show that particular care is needed when modelling non-conventional structures or in cases where there are low-emissivity surfaces or high temperature differences. It is also important that all long-wave exchange paths are considered (for example to and from windows) as some exchanges are more important than others in estimating building heating requirements. Other general conclusions from this work are as follows.

(*a*) If a complex model involving the determination of view factors is to be adopted, it is essential that they be calculated accurately, otherwise the benefit of the more detailed method may well be lost.

(*b*) If a model offers several options for the calculation of the internal long-wave radiation component, the user should be informed of the relative performance of the various algorithms.

(*c*) In many cases it seems sufficient to use a simple model. The Walton and Davies methods usually perform as well, if not better, than the more complex methods ESP(1) and DEROB, but with much faster computation times. However, both the Walton and Davies methods perform less well for non-rectangular geometries, and Walton performs less well for low-emissivity surfaces.

(*d*) Some methods are sensitive to rounding errors, and performance could be improved by using double precision in computer implementations.

(*e*) Failure to model long-wave exchange to and from windows explicitly can give errors of the order of 5% in predicted annual energy requirements. In addition, ignoring all internal long-wave radiation exchange can lead to substantial errors in annual energy requirement, particularly when exchange with windows is modelled explicitly.

Acknowledgements

P Stefanizzi gratefully acknowledges support from the Italian Consiglio Nazionale delle Ricerche while on secondment at BRE.

This work is part of the research programme of the Building Research Establishment of the UK Department of the Environment, and this paper is published by permission of the Director. The help of others in the collaborative BRE/SERC Validation project is also acknowledged.

References

1 Stefanizzi P, Wilson A and Pinney A Internal long-wave radiation exchange in buildings: Comparison of calculation methods: I Review of algorithms *Building Serv. Eng. Res. Technol.* **11**(3) 81–85 (1980)

2 Siegel R and Howell J R *Thermal Radiation Heat Transfer* (New York: McGraw-Hill) (1981)

3 Clarke J A *Energy Simulation in Building Design* (Bristol and Boston: Adam Hilger) (1985)

4 Kusuda T *NBSLD, The Computer Program for Heating and Cooling Loads in Buildings* NBS Building Science Series **69** National Bureau of Standards, USA (1976)

5 Arumi-Noe F *The DEROB System: Volume II, Explanatory Notes and Theory* Numerical Simulation Laboratory, School of Architecture, University of Texas, Austin (1979)

6 Walton G N A new algorithm for radiant interchange in room loads calculations *ASHRAE Trans.* **86**(2) 190–208 (1980)

7 Davies M G Optimal designs for star circuits for radiant exchange in a room *Building Environ.* **18**(1/2) 19–37 (1983)

8 *CIBSE Guide* Section A5 Thermal Response of Buildings (London: Chartered Institution of Building Services Engineers (1986)

9 Carroll J A A comparison of radiant interchange algorithms in *Solar Engineering—1981* (eds. R L Reid, L M Murphy and D S Ward) *Proc. ASME Solar Energy Division, 3rd Annual Conf.*, Reno, Nevada, 27 April–1 May pp 399–407 (1981)

10 Palmiter L and Wheeling T *SERIRES manual* Solar Energy Research Institute, Boulder, Colorado, USA (1983)

11 Allen E J and Pinney A A *A set of standard dwellings* BEPAC Research Report, Building Research Establishment, Watford, UK (1990)

12 Buchberg H Sensitivity of room thermal response to inside radiation exchange and surface conductance *Building Sci.* **6** 133–149 (1971)